International Journal of Climatology RMetS

Assessing the impact of El Niño–Southern Oscillation on South African temperatures during austral summer

Rakhee Lakhraj-Govender[1,2] | Stefan W. Grab[2]

[1]School of Environmental, Water and Earth Sciences, Tshwane University of Technology, Pretoria, South Africa

[2]School of Geography, Archaeology and Environmental Studies, University of the Witwatersrand, Johannesburg, South Africa

Correspondence
Rakhee Lakhraj-Govender, School of Environmental, Water and Earth Sciences, Tshwane University of Technology, 175 Nelson Mandela Drive, Arcadia Campus, Pretoria 0001, South Africa.
Email: rakhee.lg@gmail.com

Using composite analysis, the timing and extent of El Niño–Southern Oscillation (ENSO) impacts on maximum (T_{max}) and minimum temperatures (T_{min}) during austral summer are investigated for South Africa over the period 1940–2016. Pearson correlation coefficients determined between temperature data at stations within regions indicate that temperature records are coherent. During austral summer, composite analysis exhibits positive T_{max}/T_{min} anomalies for El Niño years while negative anomalies are recorded during La Niña years across all regions of South Africa. Statistical significance of composite average temperature anomalies was determined using the Student's t-test. T_{max} for El Niño years are significantly different from the neutral years over the central interior of South Africa for the period 1940–2016. The most notable finding of this study is that El Niño events have had a stronger warming effect during austral summer over many regions in South Africa after the late 1970s, than before. Such an impact has been most prominent over the northern and central interior regions, where, respectively, associated T_{max} record an average of 1.1 °C and 0.73 °C higher values for the period 1979–2016 compared to the earlier period (1940–1978). Chi-squared statistics indicate that ENSO phases exert a stronger influence on temperatures over the interior of South Africa than along the coast.

KEYWORDS

El Niño, La Niña, South Africa, surface air temperatures, teleconnections

1 | INTRODUCTION

The El Niño–Southern Oscillation (ENSO) is well known for its strong and globally distributed climatic influence. This phenomenon occurs as a product of fluctuating equatorial Pacific Ocean temperatures and large-scale air pressure changes, known as the Southern Oscillation (Bartholomew and Jin, 2013; WMO, 2014). Although ENSO phases display an irregular periodicity, the El Niño phase typically lasts a shorter duration (9–12 months) compared to La Niña phases (1–2 years; Warner and Oberheide, 2014). However, El Niño phases occur more frequently (31% of the time) than La Niña (23% of the time), while neutral conditions account for the remaining 46% of time over the period 1950–1997 (Trenberth, 1997; Welhouse *et al.*, 2016). El Niño is

generally associated with higher than usual global temperatures, while La Niña is often (but not always) linked to below normal temperatures on land (Davey *et al.*, 2014). A possible mechanism may be through the loss of heat from the ocean to the atmosphere via evaporation, which results in latent heat responsible for teleconnections (Trenberth *et al.*, 2002). Power *et al.* (1998) suggest that surface temperature changes (associated with rainfall) are forced by surface short wave radiation and latent heating, with the latter being a greater source of heating compared to the former in low-latitude regions of deep convection. Lower temperatures are associated with cloudy conditions and lower levels of incoming short-wave radiation, while higher temperatures are linked to decreased cloudiness (Jones and Trewin, 2000). El Niño and La Niña phases disturb global atmospheric

circulation, thereby affecting weather variability patterns and the probability of floods, drought, heat waves and other extreme events.

Previous studies have reported strong and coherent tele-connections between ENSO and temperature patterns, both globally (Banholzer and Donner, 2014; Cai *et al.*, 2014; WMO, 2014) and regionally (e.g., Jones and Trewin, 2000; Soltani and Gholipoor, 2006; Chowdary *et al.*, 2014). The impact of different ENSO events on regional and global temperatures is not always the same because the intensity and timing of each event varies (WMO, 2014). For instance, the 1982–1983 and 1997–1998 El Niño events severely disrupted global weather, leading to major natural disasters (e.g., floods in the eastern equatorial region of Ecuador and northern Peru) (Cai *et al.*, 2014). In addition, the strong El Niño events in 1997–1998 and 2009–2010 resulted in the years 1998 and 2010 recording global temperature departures of ~0.52 °C and 0.55 °C above the 1961–1990 long-term average, respectively (WMO, 2014). The 2015–2016 El Niño event is comparable in strength to the previous 1982–1983 and 1997–1998 strong events (WMO, 2016). This recent event increased the annual global temperature anomaly for 2016 by 0.12 °C above the 1951–1980 average (Potter *et al.*, 2017).

ENSO is known for its climatic impacts over southern Africa, with regional and inter-event variations. For instance, the 1991–1992, 2002–2003 and 2015–2016 El Niño events were associated with severe drought, while the dry conditions during the 1997–1998 El Niño were not as pronounced (e.g., Reason and Jagadheesha, 2005). Notably, Southern African ENSO studies have placed greater emphasis on the relationship between ENSO and rainfall, than on temperatures (Kruger, 1999; Reason and Rouault, 2002; Philippon *et al.*, 2012; Weldon and Reason, 2014).

Studies related to the relationship between ENSO events and South African temperatures include that by Halpert and Ropelewski (1992) who first reported teleconnections between ENSO events and southeast African temperatures. More recently, a correlation has been made between average late summer Niño3 sea surface temperatures (SSTs) and late summer temperatures (January–March) across eight stations in central South Africa (i.e., Upington, Van Wyksvlei, Armoedsvlakte, Glen College, Bloemfontein, Addo, Cedara and Emerald Dale) (Kruger and Shongwe, 2004). Findings for the relatively short period (1960–2003) of analysis report that El Niño and La Niña do not significantly influence late summer temperature increases (Kruger and Shongwe, 2004). However, Manatsa and Reason (2017) report a strong ENSO influence on maximum surface air temperature (SAT_{max}) over southern Africa during late austral summer. Despite such past investigations on the impacts of ENSO on southern African temperatures, no previous study has investigated the impact of such phases on both maximum (T_{max}) and minimum (T_{min}) temperatures using long-term quality controlled and homogenized data over the broader South African region—a gap we aim to address.

ENSO-related climate variability affects many sectors, such as human health, agriculture and water resources. Temperature and precipitation changes associated with the ENSO cycle favour the spread of insect-borne and water-borne diseases. For instance, disease outbreaks in developing countries during the 1997–1998 El Niño resulted in the loss of ca 22,000 lives (McPhaden, 2006). Rain-fed agriculture in southern Africa is also adversely impacted by ENSO-related rainfall variability, such that maize yields may decrease by up to fivefold during some El Niño events (Jury, 2002). Water resources in southern Africa become severely constrained during prolonged dry spells, and particularly those caused by El Niño events (Jury, 2002). The negative impact that ENSO events have on multiple sectors in southern Africa and beyond emphasizes the importance of effective disaster planning strategies and mitigation measures.

Meteorological organizations consider the influence of ENSO on regional weather when making seasonal forecasts, and in so doing rely upon historical climate data associated with ENSO (Chiew and MacMohan, 2002; Johnston *et al.*, 2004). ENSO is thus a relatively good predictor for seasonal forecasts in southern Africa (Manatsa and Reason, 2017). To this end, the current study aims to contribute toward an improved understanding of seasonal temperature anomalies in various subregions of South Africa, in response to ENSO phases, and hence assist future ENSO-associated forecasting.

More specifically, this paper aims to determine the impact of El Niño/La Niña phases on T_{max}/T_{min} at various localities in South Africa for the period 1940–2016, using a compositing method that averages T_{max}/T_{min} for all ENSO years during the study period. Consequently, these are used to establish the mean ENSO impact during this period, with the assumption that all ENSO events have similar characteristics and impacts (Mo, 2010). In addition, the influence that El Niño/La Niña phases have on temperature variables for the periods 1940–1978 and 1979–2016 is determined, which assists to establish possible changes in the strength of ENSO influence over time. The selection of the two periods is based on the statistical midpoint of the complete dataset (i.e., 1940–2016).

2 | METHODS

2.1 | Study area and data

The climate over southern Africa is influenced by major atmospheric operating systems such as the subtropical cyclones, jet streams and teleconnections with regional and large scale quasi-periodic climate systems (e.g., quasi-biennial oscillation [QBO], intra-seasonal waves and ENSO) (Tyson and Preston-Whyte, 2000). The warm southerly moving Mozambique and Agulhas currents play a strong

role in moderating temperatures along the east coast of southern Africa, while the cold northerly moving Benguela current has a cooling effect along the west coast of the subcontinent. South Africa's climate ranges from Mediterranean in the southwest, to temperate over the interior plateau, and subtropical in the northwest and along the northeast coast (Tyson and Preston-Whyte, 2000).

For this study, station selection is based on the availability of long-term surface temperature data with minimal gaps and with suitable spatial coverage across South Africa. These stations were grouped into regions where they have relatively close proximity to each other. Spatial coherence of stations was determined by calculating the Pearson correlation coefficients between neighbour stations (Table 3; King and Comiso, 2003). Skukuza, Warmbad and Messina stations represent the northern interior region of South Africa, while Vryburg, Marico, Kimberely, Glen College and Zuurbekom stations represent the central interior (Figure 1). Pofadder and Van Wyksvlei stations represent the western interior region, while the eastern summer rainfall region is divided into the northeast coast (i.e., Mount Edgecombe) and the northeastern interior (i.e., Cedara), each only represented by one station given the absence of reliable long-term datasets from other stations. The southeast coastal region, which receives year-round rainfall, is represented by East London and Port Elizabeth (hereafter referred to as the

southeast coast). The South African Astronomical Observatory, Cape Agulhas and Cape Columbine stations were selected to represent the winter rainfall region in the Western Cape Province (hereafter referred to as the southwest coast) (Table 1 and Figure 1). A potential limitation for such a study is the unavailability of a dense network of stations, consisting of long-term data with minimal gaps to represent a specific region. This implies that the conclusions drawn for a large area are dependent on relatively few but reliable station records. The implication is that the results may not accurately represent large regions for which no long-term or reliable station records are available. Notwithstanding the limitation of using a small number of stations to represent each region, this study provides valuable new information with regard to temperature responses to El Nino/La Nina events.

Monthly T_{max} and T_{min} for South Africa were obtained from the South African Weather Service (SAWS; Figure 1). Temperature data were quality controlled and homogenized using ProClimDB and AnClim (see Lakhraj-Govender et al., 2017). Monthly temperature anomalies were calculated by subtracting climatological means for the base period 1961–1990. Time series were detrended to remove long-term trends (an example is illustrated in Figure 2). The seasonal cycle is important for assessing the effects of ENSO (Fogt and Bromwich, 2006); hence, this study focuses on the austral summer
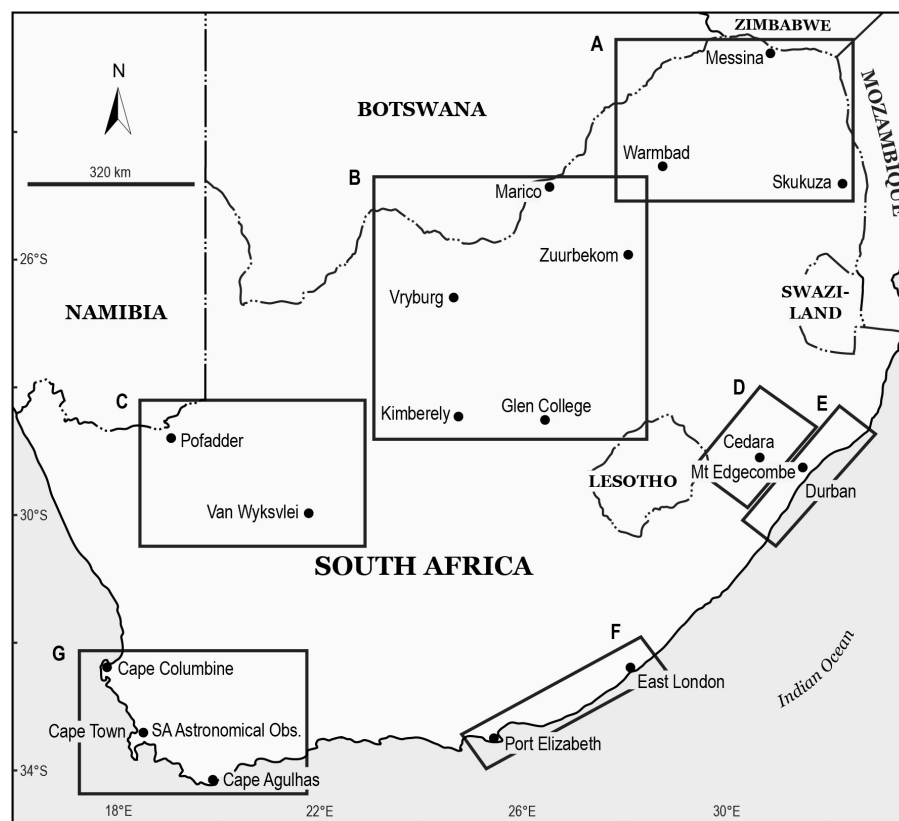

FIGURE 1 Map showing location of South African temperature stations used in this study. The boxes labelled A–G represent the different regions in South Africa. A = northern interior; B = central interior; C = western interior; D = northeastern interior; E = northeast coast; F = southeast coast; G = southwest coast
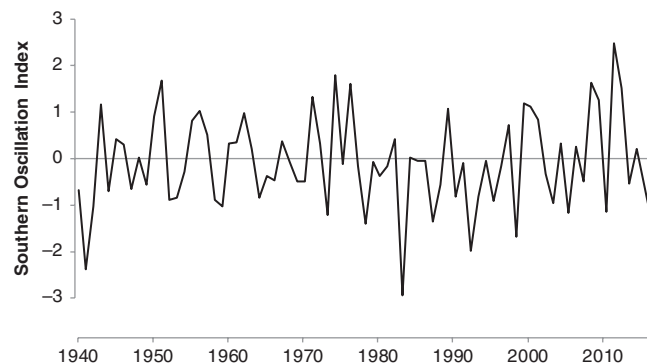
TABLE 1 South African meteorological stations used in this study, detailing GPS coordinates and start/end dates for each station

Province	Station	Start year	End year	Latitude (°S)	Longitude (°E)	Altitude (m a.s.l.)
Northern interior						
Mpumalanga	Skukuza	1941	2016	−24.99	31.59	263
Limpopo	Warmbad	1937	2016	−24.90	28.33	1,143
Limpopo	Messina	1934	2016	−22.27	29.90	538
Central interior						
Northwest	Vryburg	1920	2016	−26.95	24.65	1,234
Northwest	Marico	1934	2016	−25.50	26.35	1,078
Northern Cape	Kimberley	1940	2016	−28.80	24.80	1,196
Free State	Glen College	1915	2016	−28.95	26.33	1,303
Gauteng	Zuurbekom	1910	2016	−26.30	27.80	1,578
Western interior						
Northern Cape	Van Wyksvlei	1926	2016	−30.35	21.80	962
Northern Cape	Pofadder	1940	2016	−29.12	19.39	982
Northeastern interior						
KwaZulu-Natal	Cedara	1930	2016	−29.54	30.27	1,071
Northeast coast						
KwaZulu-Natal	Mount Edgecombe	1930	2016	−29.70	31.05	103
Southeast coast						
Eastern Cape	East London	1940	2016	−33.03	27.83	116
Eastern Cape	Port Elizabeth	1940	2016	−33.98	25.60	63
Southwest coast						
Western Cape	SA Astronom.	1933	2016	−33.56	18.28	15
Western Cape	Cape Agulhas	1884	2016	−34.49	20.01	11
Western Cape	Cape Columbine	1937	2016	−32.49	17.51	62

(December–February) which represents the peak season for El Niño and La Niña events (Cai *et al.*, 2014). Composites for El Niño and La Niña phases were calculated separately for the austral summer (3-month average of December, January and February). Monthly T_{max}/T_{min} were statistically analysed for various subregions, specifically in the context of El Niño and La Niña phases over the period 1940 to June 2016 (Table 2). According to Halpert and Ropelewski (1992), for a station to be included in composite analysis, the period of analysis must cover a minimum of five warm phases or five cold phases.

Several indices have previously been used to measure ENSO, including the normalized Tahiti minus Darwin

pressure difference (or "Troup" Southern Oscillation index [SOI]) (Jones and Trewin, 2000), multivariate ENSO index (Hänsel *et al.*, 2016) and the oceanic Niño index (ONI) (Warner and Oberheide, 2014), to name a few. The seasonal SOI is used in this study to select El Niño and La Niña events, since the index covers a longer period compared to other indices (Table 2 and Figure 3). The SOI, calculated as the difference in standardized pressure between Tahiti and Darwin, is derived from the Climate Research Unit (CRU) at the University of East Anglia in England (https://crudata.uea.ac.uk/cru/data/soi/, based on Allan *et al.*, 1991) for the period 1866–2015, while values for 2016 were obtained from the National Oceanic and Atmospheric Administration (NOAA).

2.2 | Composite

Regions with consistent SO–temperature relationships are identified using composite analysis. Recent studies (e.g., Fogt *et al.*, 2011; McAfee and Wise, 2016) have analysed composites of El Niño and La Niña phases separately, which is valuable for determining distinct features of each ENSO phase (Welhouse *et al.*, 2016). Composite analysis is considered a superior method compared to correlating ENSO teleconnections (Fogt *et al.*, 2011). Correlation does not offer insight into the magnitude of each event and is influenced by outliers (Fogt *et al.*, 2011). Thus, composites are

FIGURE 2 Southern Oscillation index for austral summer (data from https://crudata.uea.ac.uk/cru/data/soi/-)

TABLE 2 List of ENSO episode years included in this study. Southern Oscillation index (SOI), derived from the Climate Research Unit (CRU) at the University of East Anglia in England (http://www.cru.uea.ac.uk/cru/data/soi.htm, based on Allan *et al.*, 1991) for the period 1940–2016 is used to calculate austral summer SOI

El Niño	La Niña
1941, 1942, 1952, 1953, 1958, 1959, 1964, 1973, 1978, 1983, 1987, 1992, 1995, 1998, 2003, 2005, 2010, 2016	1943, 1950, 1951, 1955, 1956, 1962, 1971, 1974, 1976, 1989, 1997, 1999, 2000, 2001, 2008, 2009, 2011, 2012

used to quantify the impact of ENSO phases on temperature (Mo, 2010). However, using composites has limitations of its own, as they cannot account for differences in ENSO timing, magnitude and location, and stronger events may "overpower" the effects of weaker events (Davey *et al.*, 2014). In addition, previous composite studies have found large disparities in strength and spatial patterns between seasonal weather anomalies in the most severely affected regions during ENSO years (Chiodi and Harrison, 2013). The statistical significance of the ENSO–temperature relationship is determined using Student's *t*-test.

2.3 | Assessing temperature response to El Niño and La Niña phases through time

The selection of the two epochs (1940–1978 and 1979–2016) is based on the midpoint of the complete data set (1940–2016) for majority of stations, which coincides with the increased frequency of El Niño phases and decreased frequency of La Niña phases since the late 1970s (Kane, 2009). Monthly T_{max}/T_{min} anomalies associated with El Niño and La Niña phases were averaged for the epochs separately. The difference between the average composites for the more recent period compared to the earlier period

provides an estimate of the relative impact of ENSO for each period (i.e., 1940–1978 and 1979–2016) (Mo, 2010). A comparison of the relative ENSO impacts between the two periods is made, permitting the determination of possible changes in the strength of ENSO influence (positive or negative) through time over various subregions of South Africa.

2.4 | Contingency table and Chi-square test

The austral summer (December, January and February) is used for this part of the analysis, as this represents the period when ENSO events are fully developed (Manatsa and Reason, 2017). Temperature data were detrended using differencing, to remove the long-term trend. Twenty-five and seventy-five percent are selected as thresholds for SOI data; hence, the number of El Niño phases is the same as that for La Niña phases (i.e., 19). The T_{max}/T_{min} data for the 76-year period (1940–2016) are divided into terciles where the number of high and low years is the same (i.e., 25 years). To analyse the degree of independence of two variables (i.e., El Niño/La Niña/neutral vs. T_{max}/T_{min} anomalies), 3 × 3 contingency tables were constructed by counting the number of high/low years corresponding to El Niño/La Niña/neutral years and analysed using Chi-square test (Fogt *et al.*, 2011; Davey *et al.*, 2014). For the Chi-square test to be used with confidence, the theoretical count must be greater than 5. Given that Fisher's exact test is normally employed for data sets that are not large, this study presents the results for both these tests. The strengthening/weakening influence of the El Niño phase was also investigated for the austral summer season using the two epochs (1940–1978 and 1979–2016), as previously selected.
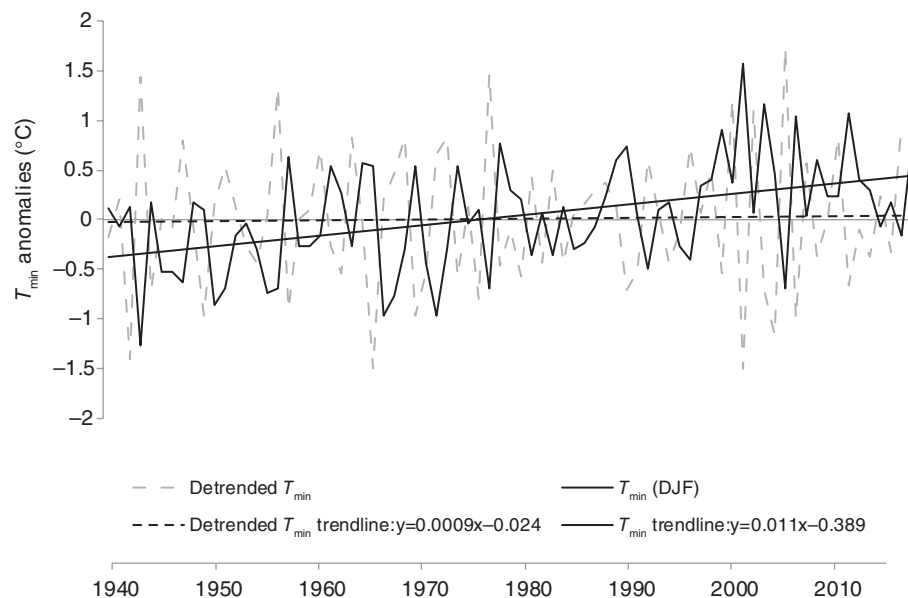

FIGURE 3 Tmin anomalies prior to and after detrending time series at Cape Columbine over the period 1940–2016

3 | RESULTS

The sections to follow present the El Niño–T_{max}/T_{min} response over the different regions, the La Niña–T_{max}/T_{min} response and finally the influence of El Niño/La Niña events through time (see Tables 3 and 4).

3.1 | Northern interior region

The correlation coefficients range from 0.89 to 0.90 for T_{max} and 0.94 to 0.97 for T_{min} between stations over the northern interior region, suggesting a high coherence of temperature variability (see Table 3). The austral summer T_{max} and T_{min} average for the selected El Niño events exhibit positive anomalies (0.81 and 0.51 °C, respectively) over the period 1940–2016 (Table 4). While a statistically significant relationship exists between El Niño–T_{max} at the Warmbad station, the remaining two stations (Skukuza and Messina) are

weakly insignificant (p-values = 0.09 and 0.08, respectively). The El Niño–T_{min} relationship is statistically significant at Warmbad and Messina. Cooling associated with La Niña events over the northern interior region record an overall negative T_{max} departure of −0.57 °C while that for T_{min} is −0.14 °C over the period 1940–2016 (Table 4).

3.2 | Central interior

For El Niño, the central interior region records correlation coefficients ranging from 0.92 to 0.98 for T_{max} and 0.95 to 0.99 for T_{min} between stations over the central interior (see Table 3). Coherent and statistically significant T_{max} positive anomalies are observed for the selected El Niño events across all five stations, with an overall positive anomaly of 1.31 °C. The El Niño–T_{min} composite is significant for three of the five stations, with an overall positive anomaly of 0.20 °C (Table 4). La Niña–T_{max} departures (−1.02 °C) are

TABLE 3 Pearson correlation coefficients between stations in each region

Northern interior					
		Messina	**Warmbad**	**Skukuza**	
Messina	T_{max}		0.89	0.90	
	T_{min}		0.97	0.94	
Warmbad	T_{max}	0.89		0.89	
	T_{min}	0.97		0.94	
Skukuza	T_{max}	0.90	0.89		
	T_{min}	0.94	0.94		
Central interior					
		Marico	Vryburg	Zuurbekom	Kimberely	Glen College
Marico	T_{max}		0.95	0.95	0.92	0.93
	T_{min}		0.98	0.97	0.96	0.97
Vryburg	T_{max}	0.95		0.94	0.98	0.98
	T_{min}	0.98		0.97	0.98	0.99
Zuurbekom	T_{max}	0.95	0.94		0.92	0.93
	T_{min}	0.97	0.97		0.95	0.97
Kimberely	T_{max}	0.92	0.98	0.92		0.98
	T_{min}	0.96	0.98	0.95		0.97
Glen College	T_{max}	0.93	0.98	0.93	0.98	
	T_{min}	0.97	0.99	0.97	0.97	
Southeast coast					
		Port Elizabeth			
East London	T_{max}	0.96			
	T_{min}	0.97			
Western interior					
		Pofadder			
Van Wyksvlei	T_{max}	0.79			
	T_{min}	0.76			
Southwest coast					
		SA Astronom.	Cape Agulhas		
Cape Columbine	T_{max}	0.95	0.92		
	T_{min}	0.91	0.91		
Cape Agulhas	T_{max}	0.95			
	T_{min}	0.97			

TABLE 4 El Niño/La Niña associated T_{max}/T_{min} anomalies over South Africa for the period 1940–2016. T_{max}/T_{min} is measured in °C

| Region | Station | Anomalies for | | | | Student's t-test | | | |
| | | El Niño | | La Niña | | El Niño | | La Niña | |
		T_{max}	T_{min}	T_{max}	T_{min}	T_{max}	T_{min}	T_{max}	T_{min}
Northeastern interior	Cedara	0.75	0.81	−0.30	−0.21	**0.00**	**0.03**	0.44	0.37
Southeast coast	East London	0.35	0.24	−0.25	−0.17	**0.04**	**0.03**	0.06	0.11
	Port Elizabeth	0.21	0.13	−0.35	−0.27	0.50	0.79	**0.03**	0.11
	Average	0.28	0.19	−0.30	−0.22				
Central interior	Zuurbekom	1.02	−1.30	−0.53	1.25	**0.02**	**0.00**	0.59	0.21
	Vryburg	1.27	0.69	−1.28	−0.48	**0.04**	**0.01**	**0.03**	0.14
	Glen College	1.73	0.62	−1.22	−0.30	**0.00**	0.09	**0.04**	0.26
	Marico	1.14	0.29	−0.80	−0.11	**0.03**	0.18	0.26	0.83
	Kimberley	1.41	0.72	−1.25	−0.50	**0.00**	**0.02**	0.06	0.13
	Average	1.31	0.20	−1.02	−0.03				
Western interior	Van Wyksvlei	0.71	0.24	−0.67	−0.12	**0.02**	0.30	**0.09**	0.75
	Pofadder	0.09	0.24	0.05	−0.07	0.49	0.42	0.54	0.86
	Average	0.40	0.24	−0.31	−0.09				
Northeast coast	Mt Edgecombe	0.22	0.30	−0.13	−0.01	0.15	**0.03**	0.63	0.62
Northern interior	Warmbath	0.82	0.21	−0.54	−0.10	**0.01**	**0.00**	0.47	0.86
	Skukuza	0.75	0.36	−0.68	−0.06	0.09	0.38	0.23	0.06
	Messina	0.85	1.00	−0.50	−0.25	0.08	**0.00**	0.44	0.78
	Average	0.81	0.51	−0.57	−0.14				
Southwest coast	SA Astronom.	0.23	0.10	−0.12	−0.12	0.38	0.71	0.60	0.34
	Cape Columbine	0.25	0.31	−0.34	−0.36	0.29	0.16	**0.05**	**0.04**
	Cape Agulhas	0.32	0.08	−0.33	−0.21	**0.01**	0.07	0.32	0.69
	Average	0.27	0.16	−0.27	−0.23				

Values in bold significant.

substantially larger compared to T_{min} departures (−0.03 °C) over the central interior for the period 1940–2016. A significantly strong and consistent relationship is observed between El Niño and T_{max} over the central interior (Table 4).

3.3 | Western interior

For El Niño, the western interior has correlation coefficients of 0.79 and 0.76 for T_{max} and T_{min}, respectively. Composite analysis displays positive T_{max} and T_{min} anomalies during El Niño events and overall negative T_{max} and T_{min} anomalies during La Niña events over the period 1940–2016. Student's t-test exhibits a statistically significant relationship for El Niño–T_{max} and La Nina–T_{max} composites at the Van Wyksvlei station (Table 4).

3.4 | Northeastern interior

For the northeastern interior, the El Niño associated T_{max}/T_{min} anomalies are significantly different from the T_{max}/T_{min} anomalies during the neutral years, indicating a strong teleconnection between El Niño events and T_{max}/T_{min}. La Niña associated T_{max}/T_{min} anomalies are insignificantly different from the anomalies during the neutral years for austral summer over the period 1940–2016 (Table 4).

3.5 | Northeast coast

During austral summer, positive T_{max} and T_{min} anomalies are recorded during El Niño events while T_{max}/T_{min} negative anomalies are observed during La Niña events over the period 1940–2016. A statistically significant relationship is evident for El Niño–T_{min} composite at the Mount Edgecombe station (Table 4).

3.6 | Southeast coast

The correlation between Port Elizabeth and East London in the southeast coast are 0.96 and 0.97 for T_{max} and T_{min}, respectively (Table 3). Average positive T_{max} and T_{min} anomalies are recorded during El Niño events while negative anomalies are observed during La Niña events over the southeast coast. Statistically significant positive T_{max} and T_{min} anomalies are observed during El Niño events at the Port Elizabeth station. The negative T_{max} anomalies associated with La Niña events are also statistically significant (Table 4).

3.7 | Southwest coast

For El Niño, the spatial coherence rates over the southwest coast range from 0.92 to 0.95 for T_{max} and 0.91 to 0.97 for

T_{min} between stations. Statistically significant positive T_{max}/T_{min} anomalies are recorded during El Niño events at Cape Agulhas, while the relationship is not significant for the remaining two stations (SA Astronomical Observatory and Cape Columbine) along the southwest coast. The overall negative T_{max} (−0.27 °C) and T_{min} (−0.23 °C) anomalies recorded over the southwest coast during La Niña events are not substantially different. Statistically significant negative T_{max} and T_{min} anomalies are observed at the Cape Columbine station during La Niña events (Table 4).

3.8 | ENSO influence on temperature through time

Average austral summer T_{max}/T_{min} anomalies during El Niño events are compared for the periods 1940–1978 and 1979–2016. A strengthening (positive) influence of El Niño events on austral summer T_{max} through time is observed across all regions of South Africa. A strengthening (positive) influence is also measured for T_{min} over the northern interior, western interior, northeast coast, southeast and southwest coasts through time. The strongest El Niño related T_{max} warming occurred over the northern interior region. Over the northern interior, El Niño associated T_{max} anomalies for austral summer increased by 1.11 °C in recent years compared to the earlier period, while associated T_{min} departures increased to a lesser extent (0.54 °C) (Table 5). Over the southeast coast, El Niño influence on T_{max} for austral

summer in recent years increased by 0.53 °C compared to the earlier period, while associated T_{min} anomalies increased to a slightly greater extent (0.55 °C). In addition, a greater strengthening influence of El Niño events on T_{max} is recorded, compared to T_{min} through time over the central interior, northeast coast, northern interior and southwest coast (Table 5). El Niño events influence T_{max} to a greater extent for the more recent period compared to earlier times over the northeastern interior (0.43 °C), northeast coast (0.29 °C) and southwest coast (0.17 °C). El Niño phases also influence T_{min} to a lesser extent for the more recent period over the central interior (−0.17) and northeastern interior (−0.39 °C) through time (Table 5).

Average austral summer T_{max}/T_{min} during La Niña events are compared for the periods 1940–1978 and 1979–2016. The earlier epoch records negative La Niña–T_{max} departures over all regions, while that for the more recent epoch varies between regions. Negative T_{max} anomalies are observed for the more recent epoch over majority of the regions, with the exception of the western interior, northeast and the southwest coasts. Over the northern interior, T_{max} and T_{min} departures associated with La Niña increased by 0.30 and 0.25 °C, respectively, between the two periods. The largest changes in T_{max} departures occurred over the central (1.34 °C) and western interior (0.68 °C) regions and the southwest coast (0.58 °C) between the two periods. For

TABLE 5 Strengthening/weakening ENSO influence on austral summer temperature anomalies through time. T_{max}/T_{min} is measured in °C

| Region | Station | El Niño | | | | | | La Niña | | | | | |
| | | 1940–1978 | | 1979–2016 | | Strengthening/ weakening | | 1940–1978 | | 1979–2016 | | Strengthening/ weakening | |
		T_{max}	T_{min}	T_{max}	T_{min}	T_{max}	T_{min}	T_{max}	T_{min}	T_{max}	T_{min}	T_{max}	T_{min}
Northeastern interior	Cedara	0.59	0.58	1.02	0.19	0.43	−0.39	−0.19	−0.38	−0.23	0.01	−0.03	0.39
Southeast coast	East London	0.09	0.05	0.58	0.42	0.50	0.37	−0.44	−0.35	−0.06	0.01	0.38	0.36
	Port Elizabeth	−0.07	−0.04	0.49	0.70	0.56	0.74	−0.07	−0.44	0.49	−0.25	0.56	0.19
	Average	0.01	0.00	0.54	0.56	0.53	0.55	−0.44	−0.35	−0.06	0.01	0.47	0.28
Central interior	Zuurbekom	0.51	−0.91	1.54	−1.69	1.03	−0.77	−0.73	1.44	−0.33	1.05	0.40	−0.39
	Vryburg	1.18	0.69	1.36	0.68	0.18	−0.01	−2.21	−0.76	−0.35	−0.20	1.86	0.55
	Glen College	1.30	0.49	2.16	0.74	0.86	0.25	−2.06	−0.54	−0.38	−0.05	1.67	0.48
	Marico	0.67	0.40	1.62	0.19	0.96	−0.21	−1.44	−0.13	−0.17	−0.08	1.27	0.05
	Kimberley	1.20	0.81	1.85	0.69	0.64	−0.12	−2.00	−0.86	−0.51	−0.14	1.49	0.72
	Average	0.97	0.30	1.70	0.12	0.73	−0.17	−1.69	−0.17	−0.35	0.12	1.34	0.28
Western interior	Van Wyksvlei	0.40	0.04	1.03	0.44	0.63	0.41	−1.20	−0.17	−0.14	−0.06	1.07	0.11
	Pofadder	0.23	0.14	−0.04	0.33	−0.27	0.19	−0.1	0.11	0.20	−0.25	0.30	−0.36
	Average	0.31	0.09	0.50	0.39	0.18	0.30	−0.65	−0.03	0.03	−0.15	0.68	−0.12
Northeast coast	Mt Edgecombe	0.08	0.17		0.37	0.29	0.26	−0.37	−0.22	0.12	0.2	0.49	0.42
Northern interior	Warmbath	0.98	1.05	1.59	0.42	0.61	−0.63	−0.79	−0.18	−0.28	−0.03	0.51	0.15
	Skukuza	0.13	0.34	1.37	0.38	1.24	0.04	−0.31	−0.57	−0.77	−0.23	−0.46	0.34
	Messina	0.18	0.51	1.29	1.05	1.11	0.54	−0.93	−0.38	−0.08	−0.12	0.85	0.26
	Average	0.18	0.51	1.29	1.05	1.11	0.54	−0.68	−0.37	−0.38	−0.13	0.30	0.25
Southwest coast	SA Astronom.	0.31	0.03	0.15	0.18	−0.15	0.15	−0.48	−0.24	0.25	0.00	0.73	0.24
	Cape Columbine	0.14	0.05	0.36	0.10	0.22	0.05	−0.47	−0.53	−0.22	−0.20	0.25	0.33
	Cape Agulhas	0.1	0.14	0.54	0.38	0.44	0.24	−0.72	−0.03	0.05	−0.12	0.77	−0.09
	Average	0.18	0.07	0.35	0.22	0.17	0.15	−0.56	−0.27	0.03	−0.11	0.58	0.16

La Niña events, T_{min} increased in magnitude over the northeast coast (0.42 °C), northeastern interior (0.39 °C), central interior (0.28 °C), southeast (0.28 °C) and southwest (0.16 °C) coasts through time (Table 5). However, the western interior recorded a decreasing T_{min} departure (−0.12 °C) through time (Table 5).

3.9 | Chi-square test results

The results associated with the Chi-square test for the austral summer (December, January and February) display p-values lower than the significance level of 0.05 for all stations in the northern and central interior of South Africa. This indicates that El Niño/La Niña and T_{max}/T_{min} are not independant, again emphasizing the influence of these ENSO phases on temperature over the interior (Table 6). However, at Messina, Glen College and Skukuza, the p-values are higher than 0.05 for T_{min}, indicating that El Niño/La Niña phases do not influence T_{min}. Significant ENSO associations are also recorded at Van Wyksvlei, Cedara and Cape Columbine for T_{max} and Mt. Edgecombe for T_{min}. Although T_{max} at Marico and T_{min} at Zuurbekom and Messina recorded counts of below 5, the Fisher's exact test corresponded to the p-value for Chi-square test in all instances (Table 6). A strengthening El Niño influence on T_{max} is also recorded for the majority of stations across South Africa, with the exception of the SA Astronomical Observatory and Pofadder stations. A larger proportion of stations record a weakening influence of the El Niño phase on T_{min} (namely Cedara, Zuurbekom, Vryburg, Marico, Kimberely and Warmbad) with time.

4 | DISCUSSION

South African surface air temperatures are influenced by both phases of ENSO. The most significant responses to El Niño events occur over the central interior region during austral summer for both T_{max} and T_{min} over the period 1940–2016 (Table 4). The central interior region displays the strongest response to El Niño events in terms of the magnitude of the positive anomaly (1.31 °C), while the northern interior region exhibits the second strongest response (0.81 °C). Globally, the region most directly affected by the Southern Oscillation is the tropics (i.e., including all areas within 20°N/S of the equator) (Halpert and Ropelewski, 1992). In addition, the lag surface air temperature response to El Niño events is slightly less in the tropics than other regions of the world (Trenberth et al., 2002). It is thus expected that South African stations in closest proximity to the tropics (i.e., northern and central interior regions) would experience a stronger response to El Niño events, compared to regions further south. In addition, the interior is more likely to show a stronger ENSO/temperature response than coastal regions given reduced oceanic climatic moderating effects over the interior. T_{min} response to El Niño events

exhibit smaller positive anomalies compared to T_{max} responses across all regions. This may be owing to reduced cloudiness during El Niño events, which results in warmer daytime and cooler night temperatures (Ashcroft et al., 2014). The reverse is true for La Niña events; these reflect larger negative anomalies for T_{max} and smaller T_{min} negative anomalies. The observed T_{min} response is possibly due to the influence of T_{max} on T_{min}, particularly during the warmer months when T_{min} are more strongly influenced by T_{max} from the previous day (Jones and Trewin, 2000; Ashcroft et al., 2014).

The strength of the El Niño–temperature relationship is influenced by the distance between the Pacific Ocean and South Africa, as also the various stages of an ENSO event in the Pacific Ocean (Lee and Julien, 2016). A typical El Niño event in the Pacific Ocean undergoes antecedent conditions in September (−), an early stage of warming (onset phase) during December (−1) and the peak phase during April (0) (i.e., just before the maximum temperature occurs near the Equator-Peru coast) (Rasmusson and Carpenter, 1982). This is followed by the transition phase in September (0), which is the end of the first pronounced decrease in SSTs, and finally the mature stage during January (+1), when composite SSTs decrease along the Ecuador/Peru coast and approach normal (Rasmusson and Carpenter, 1982). However, the weather/climatic consequences of each El Niño event are not identical given that these depend on the intensity of the event, the time of year when the event develops and the interaction with other climate dynamics (WMO, 2014). Previous climate studies on southeastern Africa noted above median T_{mean} for El Niño phases starting in October (0), with the detected signal period extending to June (+) following El Niño phases for the period 1880–1988 (Halpert and Ropelewski, 1992). The differences in the signal periods selected by this study and that of Halpert and Ropelewski (1992) may arise from the different periods of observation, temperature variables used, and stations selected. In addition, Jones and Trewin (2000) note that the greatest temperature impact of ENSO in Australia is on T_{mean}, rather than other temperature variables, such as diurnal temperature range. We therefore investigate the impact of El Niño/La Niña events on austral summer T_{max} and T_{min}.

For La Niña events, earlier studies report below normal T_{mean} for the period August (0)–June (+) over southeastern Africa for the period 1880–1988 (Halpert and Ropelewski, 1992). Previous studies also noted the difficulty in determining La Niña related responses due to the occurrence of El Niño and La Niña in subsequent years (e.g., Dracup and Kahya, 1994). Previous studies record increased magnitudes of El Niño events since the mid-1970s (Haines et al., 2000), which possibly overwhelmed the La Niña–temperature response. Also noteworthy is that climate change may alter the frequency and magnitude of the ENSO cycle (Haines et al., 2000). Modelling studies indicate that anthropogenic

TABLE 6 Regional Chi-square statistics for traditional summer T_{max}/T_{min} anomalies (average of December, January and February), rate of occurrence and strengthening/weakening influence of El Niño phases on T_{max}/T_{min}. Chi-square critical value = 9.48 degree of freedom = 4 and p-values in bold are significant. High T_{max}/T_{min} = the upper tercile, medium T_{max}/T_{min} = middle 25 years of temperature data and low T_{max}/T_{min} = the lower tercile representing the last 25 years of temperature data

Region	Station / T_{max}/T_{min}	Chi-square (observed value)	p-value	Fisher's exact	Rates of high T_{max}/T_{min} occurrence for El Niño years	Rates of low T_{max}/T_{min} occurrence for La Niña years	Strengthening/ weakening influence of El Niño on T_{max}/T_{min} [a]	Phase	High T_{max}	Medium T_{max}	Low T_{max}	Phase	High T_{min}	Medium T_{min}	Low T_{min}
Northeastern interior	Cedara														
	T_{max}	13.286	**0.010**	0.011	0.61	0.50	0.43	El Niño	11	6	1	El Niño	10	5	3
	T_{min}	6.836	0.145	0.079	0.56	0.44	−0.39	La Nia	3	6	9	La Niña	4	8	6
								Neutral	10	17	14	Neutral	10	16	15
Southeast coast	East London														
	T_{max}	5.238	0.264	0.28	0.39	0.50	0.50	El Niño	7	5	6	El Niño	8	7	3
	T_{min}	5.336	0.255	0.29	0.44	0.50	0.37	La Niña	4	5	9	La Niña	4	5	9
								Neutral	13	18	9	Neutral	12	16	12
	Port Elizabeth														
	T_{max}	7.002	0.136	0.129	0.22	0.22	0.41	El Niño	2	9	7	El Niño	4	8	6
	T_{min}	2.051	0.726	0.722	0.11	0.17	0.11	La Niña	9	6	3	La Niña	7	7	4
								Neutral	13	14	14	Neutral	14	13	14
Central interior	Zuurbekom														
	T_{max}	10.012	**0.040**	0.048	0.50	0.33	1.03	El Niño	9	6	3	El Niño	11	5	2
	T_{min}	11.035	**0.026**	0.032	0.61	0.39	−0.77	La Niña	1	11	6	La Niña	5	6	7
								Neutral	9	22	10	Neutral	8	17	16
	Vryburg														
	T_{max}	11.947	**0.018**	0.022	0.56	0.56	0.03	El Niño	10	6	2	El Niño	11	4	3
	T_{min}	13.137	**0.011**	0.011	0.61	0.44	−0.22	La Niña	10	6	10	La Niña	1	9	8
								Neutral	12	17	12	Neutral	12	16	13
	Glen College														
Central interior	T_{max}	15.992	**0.003**	0.002	0.61	0.61	0.86	La Niña	2	5	11	El Niño	9	6	3
	T_{min}	5.935	0.204	0.231	0.5	0.44	0.25	Neutral	10	12	18	La Niña	5	6	8
								El Niño	11	6	1	Neutral	10	18	13
	Marico														
	T_{max}	12.048	**0.017**	0.016	0.56	0.50	0.96	La Niña	2	5	11	La Niña	3	9	6
	T_{min}	10.641	**0.031**	0.043	0.61	0.33	−0.21	Neutral	10	7	9	Neutral	7	17	14
								El Niño	10	19	1	El Niño	11	3	2
	Kimberley														
	T_{max}	25.229	**<0.0001**	<0.0001	0.67	0.67	0.64	El Niño	12	6	0	El Niño	10	6	1
	T_{min}	10.442	**0.034**	0.027	0.56	0.44	−0.12	La Niña	1	5	12	La Niña	5	5	8
								Neutral	11	18	12	Neutral	9	17	15
Western interior	Van Wyksvlei														
	T_{max}	9.163	**0.057**	0.067	0.44	0.63	0.63	El Niño	8	7	3	El Niño	8	6	4
	T_{min}	2.479	0.648	0.672	0.44	0.41	0.41	La Niña	5	3	10	La Niña	5	6	7
								Neutral	11	19	11	Neutral	11	17	13
	Pofadder														
	T_{max}	3.326	0.505	0.512	0.44	0.44	−0.02	El Niño	8	2	8	El Niño	6	6	6
	T_{min}	2.403	0.662	0.665	0.33	0.44	0.33	La Niña	4	6	8	La Niña	4	6	8
								Neutral	13	10	18	Neutral	14	16	10

TABLE 6 (Continued)

Region	Station/ T_{max}/T_{min}	Chi-square (observed value)	p-value	Fisher's exact	Rates of high T_{max}/T_{min} occurrence for El Niño years	Rates of low T_{max}/T_{min} occurrence for La Niña years	Strengthening/ weakening influence of El Niño on T_{max}/T_{min} [a]		High T_{max}	Medium T_{max}	Low T_{max}		High T_{min}	Medium T_{min}	Low T_{min}
Northeast coast	Mt Edgecombe														
	T_{max}	5.907	0.206	0.180	0.39	0.44	0.29	El Niño	7	9	2	El Niño	10	7	1
								La Niña	6	4	8	La Niña	7	5	6
								Neutral	11	15	14	Neutral	7	17	17
	T_{min}	12.233	**0.016**	0.011	0.56	0.33	0.26								
Northern interior	Warmbad							El Niño	12	4	2	El Niño	9	9	0
	T_{max}	16.289	**0.003**	0.005	0.67	0.5	0.61	La Niña	2	8	8	La Niña	3	9	6
	T_{min}	13.504	**0.009**	0.003	0.44	0.33	−0.63	Neutral	9	18	14	Neutral	11	12	18
	Skukuza							El Niño	11	6	1	El Niño	6	6	6
	T_{max}	9.777	**0.044**	0.040	0.61	0.39	1.24	La Niña	4	7	7	La Niña	6	4	8
	T_{min}	3.800	0.434	0.426	0.33	0.44	0.04	Neutral	10	15	16	Neutral	12	19	10
	Messina							El Niño	11	3	4	El Niño	9	8	1
	T_{max}	13.440	**0.009**	0.013	0.61	0.5	1.11	La Niña	2	7	9	La Niña	9	7	2
	T_{min}	8.224	0.084	0.089	0.50	0.5	0.54	Neutral	11	19	11	Neutral	12	15	14
Southwest coast	SA Astronom.							El Niño	7	8	3	El Niño	7	6	5
	T_{max}	2.518	0.641	0.627	0.39	0.39	−0.15	La Niña	5	6	7	La Niña	5	4	9
	T_{min}	5.226	0.265	0.291	0.39	0.5	0.15	Neutral	12	14	14	Neutral	12	19	10
	Cape Columbine							El Niño	7	9	2	El Niño	10	5	3
	T_{max}	10.211	**0.037**	0.062	0.50	0.56	0.22	La Niña	2	7	9	La Niña	1	8	9
	T_{min}	3.880	0.422	0.021	0.44	0.44	0.40	Neutral	15	13	13	Neutral	13	15	12
	Cape Agulhas							El Niño	9	5	4	El Niño	8	6	4
	T_{max}	3.956	0.412	0.437	0.50	0.56	0.44	La Niña	4	4	10	La Niña	3	7	8
	T_{min}	6.880	0.142	0.056	0.44	0.44	0.06	Neutral	11	20	10	Neutral	13	16	12

[a] The difference between the T_{max}/T_{min} anomalies for El Niño phases for the periods 1940–1978 and 1979–2016.

climate change and increased greenhouse gas emissions may change the strength and position of ENSO teleconnection patterns (Sun *et al.*, 2016). However, coupled ocean atmosphere models produce disparate outcomes on ENSO amplitudinal changes and spatial patterns in response to climate change (Zhou *et al.*, 2014). While several studies (e.g., Zhou *et al.*, 2014; Sun *et al.*, 2016; Jiang *et al.*, 2018) have investigated global warming-induced changes in ENSO teleconnections for different regions of the world, such an analysis has been largely absent for the southern African region.

The destructive environmental and socio-economic impacts of ENSO demand an improved understanding of how ENSO and its influence on temperature will change under greenhouse warming conditions (Kim *et al.*, 2014). Hence, our investigation on the relative strength of ENSO's influence on T_{max} and T_{min} through time take into account regional warming. The 1976/1977 climatic shift of ENSO activity resulted in more frequent El Niño phases after 1976 (Trenberth *et al.*, 2002). The influence of El Niño phases on T_{max} strengthens when comparing the period 1940–1978 with 1979–2016 across all regions of South Africa (see Table 5). Manatsa *et al.* (2018) suggest that post-1998, T_{min} was suppressed and T_{max} enhanced, resulting in an increase in diurnal temperature which discouraged low-level clouds. Consequently, more solar energy reaches the earth's surface and increases T_{max}. However, with the exception of the northeastern and central interior regions, we also observe a strengthening influence of El Niño events on T_{min} across all regions.

A previous investigation of ENSO impacts on the Western Cape summer climate and SSTs, where prevailing southeasterly winds drive coastal upwelling, found that wind speed is weaker (stronger) than normal during El Niño (La Niña) phases leading to changes in SSTs (Rouault *et al.*, 2010). Notably, the growing influence of El Niño events on T_{max} through time is stronger over the northern (1.11 °C) and central (0.73 °C) interior regions than all other regions tested in this study (see Table 5). Using a simple dynamical model, it seems that the ENSO signal emerging from the tropics was three times stronger in amplitude over the period 1978–1997 compared with 1958–1977 (Greatbatch *et al.*, 2004). Mo (2010) suggests that changes to the climatic impacts associated with ENSO are possibly related to recent changes in the number of El Niño/La Niña events and/or the changing behaviour of ENSO under global warming conditions. More recently, Sun *et al.* (2016) observed a stronger influence of ENSO on summer surface temperatures over western Russia and suggest that the enhancement of ENSO teleconnections could be attributed to a change in the ENSO-related tropical thermal forcing after 1980.

With the exception of the northeastern interior, all other regions across South Africa record warmer T_{max} during La Niña events during the period 1979–2016 than earlier period 1940–1978. Hence, the cooling influences of La Niña events on T_{max} have weakened during austral summer over the last few decades. The greatest temporal decrease in T_{max} during La Niña occurs over the northeastern interior (Table 5). This is possibly due to stronger warming trends observed for the more recent epoch, which also coincides with an intensification of the warm Agulhas current along the east coast of the country (Rouault *et al.*, 2010). The cooling influence of La Niña events on T_{min} also strengthens through time over the western interior, while a decreasing influence is recorded across all other regions (Table 5). This might, in part, be owing to a reduced frequency of La Niña events since the late 1970s (Kane, 2009). As also suggested by Larkin and Harrison (2005), the implication of such findings is that composites for more recent decades should take preference for seasonal forecasting than those for earlier ENSO events, which no longer serve as adequate indicators for future climate.

The results presented have important implications for future research on ENSO–temperature relationships in South Africa, given that little is known about the physical processes responsible for surface temperature signals, such as the role of water vapour, clouds and land surface properties (Zhang *et al.*, 2011). ENSO events impact on global mean surface air temperature because of heat exchanges across ocean–atmosphere–land boundaries (Trenberth *et al.*, 2002; McPhaden *et al.*, 2015), however, the physical mechanism responsible for ENSO's influence on climate over South Africa is still largely unknown (Boulard *et al.*, 2013). Recently though, Manatsa *et al.* (2018) suggest ENSO teleconnection is mostly achieved through regulation of cloud cover. It is also understood that the response of ENSO is dependent on the phase of the Madden–Julian oscillation (MJO) over the Northern Hemisphere (Shimizu *et al.*, 2016). However, it is still not fully understood how the combined effects of ENSO and MJO manifest climatically over the Southern Hemisphere (Shimizu *et al.*, 2016). In addition, QBO, quasi-triennial oscillations (QTO) and the Southern Annular Mode (SAM) may influence the impact of ENSO events on temperature (Kane, 2009; Fogt *et al.*, 2011), and these need to be further investigated in combination with ENSO.

5 | CONCLUSION

This paper demonstrates the importance of assessing the impacts of El Niño and La Niña events on T_{max}/T_{min} independently for different regions of South Africa. The variety of T_{max}/T_{min} responses to El Niño/La Niña events (magnitude and timing) for the different regions have important implications for regional disaster planning, given the destructive environmental consequences of ENSO events. Most notable is the strengthening/weakening influence of El Niño/La Niña events on T_{max} and T_{min} when comparing the periods 1940–1978 with 1979–2016. The strengthening

influence of El Niño on T_{max} during austral summer through time occurs across all regions of South Africa. Further studies are required to help improve the understanding of ENSO teleconnections in the Southern Hemisphere and determine whether changes in these teleconnections are a result of global warming or internal decadal climate variability (Sun *et al.*, 2016).

ORCID

Rakhee Lakhraj-Govender https://orcid.org/0000-0003-1177-5023
Stefan W. Grab https://orcid.org/0000-0001-7678-1526

REFERENCES

Allan, R.J., Nicholls, N., Jones, P.D. and Butterworth, I.J. (1991) A further extension of the Tahiti-Darwin SOI, early SOI results and Darwin pressure. *Journal of Climate*, 4, 743–749.

Ashcroft, L., Karoly, D.J. and Gergis, J. (2014) Southeastern Australian climate variability 1860–2009: a multivariate analysis. *International Journal of Climatology*, 34, 1928–1944.

Banholzer, S. and Donner, S. (2014) The influence of different El Niño types on global average temperature. *Geophysical Research Letters*, 41, 2093–2099.

Bartholomew, H. and Jin, S. (2013) ENSO effect on land skin temperature variations: a global study from satellite remote sensing and NCEP/NCAR reanalysis. *Climate*, 1, 53–73.

Boulard, D., Pohl, B., Cretat, J., Vigaud, N. and Pham-Xuan, T. (2013) Downscaling large-scale climate variability using a regional climate model: the case of ENSO over southern Africa. *Climate Dynamics*, 40, 1141–1168.

Cai, W., Borlace, S., Lengaigne, M., van Rensch, P., Collins, M., Vecchi, G., Timmermann, A., Santoso, A., McPhaden, M.J., Wu, L., England, M.H., Wang, G., Guilyardi, E. and Jin, F. (2014) Increasing frequency of extreme El Niño events due to greenhouse warming. *Nature Climate Change*, 4, 111–116.

Chiew, F.H.S. and MacMohan, T.A. (2002) Global ENSO–streamflow teleconnection, streamflow forecasting and interannual variability. *Hydrological Sciences Journal*, 47, 505–522.

Chiodi, A.M. and Harrison, D.E. (2013) El Niño impacts on seasonal U.S. atmospheric circulation, temperature, and precipitation anomalies: The OLR-Event perspective. *Journal of Climate*, 26, 822–837.

Chowdary, J.S., John, N. and Gnanaseelan, C. (2014) Interannual variability of surface air-temperature over India: impact of ENSO and Indian Ocean sea surface temperature. *International Journal of Climatology*, 34, 416–429.

Davey, M.K., Brookshaw, A. and Ineson, S. (2014) The probability of the impact of ENSO on precipitation and near-surface temperature. *Climate Risk Management*, 1, 5–24.

Dracup, J.A. and Kahya, E. (1994) The relationships between US streamflow and La Niña events. *Water Resources Research*, 30, 2133–2141.

Fogt, R.L. and Bromwich, D.H. (2006) Decadal variability of the ENSO teleconnection to the high-latitude South Pacific governed by coupling with the South Annular Mode. *Journal of Climate*, 19, 979–997.

Fogt, R.L., Bromwich, D.H. and Hines, K.M. (2011) Understanding the SAM influences on the South Pacific–ENSO teleconnection. *Climate Dynamics*, 36, 1555–1576.

Greatbatch, R.J., Lu, J. and Peterson, K.A. (2004) Nonstationary impact of ENSO on Euro-Atlantic winter climate. *Geophysical Research Letters*, 31, L02208. https://doi.org/10.1029/2003GL018542.

Haines, A., McMichael, A.J. and Epstein, P.R. (2000) Environment and health: global climate change and health. *Canadian Medical Association Journal*, 163, 729–734.

Halpert, M.S. and Ropelewski, C.F. (1992) Surface temperature pattern associated with Southern Oscillation. *Journal of Climate*, 5, 577–593.

Hänsel, S., Medeiros, D.M., Matschullat, J., Petta, R.A. and de Mendonça Silva, I. (2016) Assessing homogeneity and climate variability of temperature and precipitation series in the capitals of north-eastern Brazil. *Frontiers Earth Science*, 4, 1–21. https://doi.org/10.3389/feart.2016.00029.

Jiang, W., Huang, G., Huang, P. and Hu, K. (2018) Weakening of northwest Pacific anticyclone anomalies during post-El Niño summers under global warming. *Journal of Climate*, 31, 3539–3555. https://doi.org/10.1175/JCLI-D-17-0613.1.

Johnston, P.A., Archer, E.R.M., Vogel, C.H., Bezuidenhout, C.N., Tennant, W.J. and Kuschke, R. (2004) Review of seasonal forecasting in South Africa: producer to end user. *Climate Research*, 28, 67–82.

Jones, D.A. and Trewin, B.C. (2000) On the relationship between the El Niño–Southern Oscillation and Australian land surface temperature. *International Journal of Climatology*, 20, 697–719.

Jury, M.R. (2002) Economic impacts of climate variability in South Africa and development of resource prediction Models. *Journal of Applied Meteorology*, 41, 46–55.

Kane, R.P. (2009) Periodicities, ENSO effects and trends of some South African rainfall series: an update. *South African Journal of Science*, 105, 199–207.

Kim, S.T., Cai, W., Jin, F., Santoso, A., Wu, L., Guilyardi, E. and An, S. (2014) Response of El Niño sea surface temperature variability to greenhouse warming. *Nature Climate Change*, 4, 786–790.

King, J.C. and Comiso, J.C. (2003) The spatial coherence of interannual temperature variations in the Antarctic Peninsula. *Geophysical Research Letters*, 30, 1040. https://doi.org/10.1029/2002GL015580.

Kruger, A.C. (1999) The influence of the decadal-scale variability of summer rainfall on the impact of El Niño phase and La Niña events in South Africa. *International Journal of Climatology*, 19, 59–68.

Kruger, A.C. and Shongwe, S. (2004) Temperature trends in South Africa: 1960–2003. *International Journal of Climatology*, 24, 1929–1945.

Lakhraj-Govender, R., Grab, S. and Ndebele, N.E. (2017) A homogenized long-term record for the Western Cape Province in South Africa: 1916-2013. *International Journal of Climatology*, 37, 2337–2357.

Larkin, N.K. and Harrison, D.E. (2005) Global seasonal temperature and precipitation anomalies during El Niño autumn and winter. *Geophysical Research Letters*, 32, L16705. https://doi.org/10.1029/2005GL022860.

Lee, J.H. and Julien, P.Y. (2016) ENSO impacts on temperature over South Korea. *International Journal of Climatology*, 36, 3651–3663.

Manatsa, D. and Reason, C. (2017) ENSO–Kalahari Desert linkages on southern Africa summer surface air temperature variability. *International Journal of Climatology*, 37, 1728–1745.

Manatsa, D., Mukwada, G. and Makaba, L. (2018) ENSO shifts and their link to southern Africa surface air temperature in summer. *Theoretical and Applied Climatology*, 132, 727–738.

McAfee, S.A. and Wise, E.K. (2016) Intra-seasonal and inter-decadal variability in ENSO impacts on the Pacific Northwest. *International Journal of Climatology*, 36, 508–516.

McPhaden, M.J. (2006) ENSO as an integrating concept in earth science. *Science*, 314, 1740–1745.

McPhaden, M.J., Timmermann, A., Widlansky, M.J., Balmaseda, M.A. and Stockdale, T.N. (2015) The curious case of the El Niño that never happened: a perspective from 40 years of progress in climate research and forecasting. *Bulletin of the American Meteorological Society*, 96, 1647–1665.

Mo, K.C. (2010) Interdecadal modulation of the impact of ENSO on precipitation and temperature over the United States. *Journal of Climate*, 23, 3639–3656.

Philippon, N., Rouault, M., Richard, Y. and Favre, A. (2012) The influence of ENSO on winter rainfall in South Africa. *International Journal of Climatology*, 32, 2333–2347.

Potter, S., Cabbage, M. and McCarthy, L. (2017) *NASA, NOAA data show 2016 warmest year on record globally*. New York, NY: Goddard Institute for Space Studies. Available at: https://www.nasa.gov/press-release/nasa-noaa-data-show-2016-warmest-year-on-record-globally [accessed 22nd January 2017].

Power, S., Tseitkin, F., Torok, S., Lavery, B., Dahni, R. and McAvaney, B. (1998) Australian temperature, Australian rainfall and the Southern Oscillation, 1910-1992: coherent variability and recent changes. *Australian Meteorological Magazine*, 47, 85–101.

Rasmusson, E.M. and Carpenter, T.H. (1982) Variations in tropical sea surface temperature and surface wind fields associated with the Southern Oscillation/El Niño. *Monthly Weather Review*, 110, 354–384.

Reason, C.J.C. and Jagadheesha, D. (2005) A model investigation of recent ENSO impacts over southern Africa. *Meteorology and Atmospheric Physics*, 89, 181–205.

Reason, C.J.C. and Rouault, M. (2002) ENSO-like decadal variability and South African rainfall. *Geophysical Research Letters*, 29, 1638–1641.

Rouault, M., Pohl, B. and Penven, P. (2010) Coastal oceanic climate change and variability from 1982 to 2009 around South Africa. *African Journal of Marine Science*, 32, 237–246.

Shimizu, M.H., Ambrizzi, T. and Liebmann, B. (2016) Extreme precipitation events and their relationship with ENSO and MJO phases over northern South America. *International Journal of Climatology*, 37, 2977–2989.

Soltani, A. and Gholipoor, M. (2006) Teleconnections between El Niño/Southern Oscillation and rainfall and temperature in Iran. *International Journal of Agricultural Research*, 1, 603–608.

Sun, C., Li, J. and Ding, R. (2016) Strengthening relationship between ENSO and western Russian summer surface temperature. *Geophysical Research Letters*, 43, 843–851.

Trenberth, K. (1997) The definition of El Niño. *Bulletin of the American Meteorological Society*, 78, 2771–2777.

Trenberth, K.E., Caron, J.M., Stepaniak, D.P. and Worley, S. (2002) Evolution of El Niño–Southern Oscillation and global atmospheric surface temperature. *Journal of Geophysical Research*, 107, 5–12.

Tyson, P.D. and Preston-Whyte, R.A. (2000) *The Weather and Climate of Southern Africa*. Cape Town: Oxford University Press.

Warner, K. and Oberheide, J. (2014) Nonmigrating tidal heating and MLT tidal wind variability due to the El Niño–Southern Oscillation. *Journal of Geophysical Research: Atmospheres*, 119, 1249–1265.

Weldon, D. and Reason, C.J.C. (2014) Variability of rainfall characteristics over the south coast region of South Africa. *Theoretical and Applied Climatology*, 115, 177–185.

Welhouse, L.J., Lazzara, M.A., Keller, L.M., Tripoli, G.J. and Hitchman, M.H. (2016) Composite analysis of the effects of ENSO on Antarctica. *Journal of Climate*, 29, 1797–1808.

WMO. (2014) *El Niño/Southern Oscillation*, Vol. 1145. Geneva: WMO, pp. 2–4. Available online http://www.wmo.int/pages/prog/wcp/wcasp/documents/JN142122_WMO1145_EN_web.pdf [accessed 27th June 2016].

WMO. (2016) *El Niño/La Niña May 2016 update*. Geneva: WMO. Available at: http://www.wmo.int/pages/prog/wcp/wcasp/enso_update_latest.html [Accessed 20th April 2016].

Zhang, T., Hoerling, M.P., Perlwitz, S.D. and Murray, D. (2011) Physics of U.S. surface temperature response to ENSO forcing. *Journal of Climate*, 24, 4874–4887.

Zhou, Z.Q., Xie, S.P., Zheng, X.T., Liu, Q. and Wang, H. (2014) Global warming-induced changes in teleconnections over the North Pacific and North America. *Journal of Climate*, 27, 9050–9064.